J. Chem. Sci. Vol. 125, No. 6, November 2013, pp. 1629–1637.

First principle study of the interaction of elemental Hg with small neutral, anionic and cationic Pd_n (n = 1–6) clusters

SHAMOON AHMAD SIDDIQUI[a,b,*] and NADIR BOUARISSA[a,b]

[a]Department of Physics, College of Arts and Science, [b]Promising Centre for Sensors and Electronic Devices, Najran University, Najran P.O. Box 1988, Kingdom of Saudi Arabia
e-mail: shamoonasiddiqui@gmail.com

MS received 9 March 2013; revised 8 June 2013; accepted 12 August 2013

Abstract. Density functional theory (DFT)-based calculations have been performed so as to study the interaction of elemental mercury (Hg) with small neutral, cationic and anionic palladium clusters (Pd_n, n = 1–6). Results of these calculations clearly indicate that frontier molecular orbital (FMO) theory is a useful method to predict the selectivity of Hg adsorption. Binding energies of Hg on cationic Pd_n clusters are generally found to be greater than those on neutral and anionic clusters. Results of natural bond orbital (NBO) analysis show that the flow of electrons in the neutral and charged complexes is mainly due to s orbitals of Hg. NBO analysis also indicates that, in most of the cases, the binding energies of Hg with Pd_n clusters are directly proportional to charge transfer, i.e., greater the charge transfer, higher is the binding energy.

Keywords. Detection of elemental mercury; frontier molecular orbital (FMO) theory; density functional theory (DFT).

1. Introduction

Gasification of coal is a commercially important method for utilization of coal reserves. This technique has been successfully used in integrated gasification combined cycle (IGCC) power plants. The fuel gas generated from coal gasification contains low concentrations of elemental mercury (Hg),[1,2] which may lead to environmental as well as technical problems during fuel gas utilization. This is due to the fact that, Hg is well-known as highly toxic and has adverse effect on the central nervous system, which may led to blindness, pulmonary disease, renal failure, chromosome damage and severe respiratory damage.[3] There is increasing concern over environmental Hg pollution across the globe, which has led to many legislative acts, one of which is the United States Environmental Protection Agency's Clean Air Mercury Rule. We can find three types of Hg in environment, which are elemental, inorganic and organic Hg. Nevertheless, because of low melting point, high equilibrium pressure and low solubility in water, elemental Hg is very difficult to remove from the fuel gases.[4] Hg removal from fuel gas using sorbents is an attractive method for Hg control. A large number of sorbents, in particular activated carbon, was proved to be effective for elemental Hg capture at low temperatures, however, these sorbents are much less effective at high temperatures (>200°C).[5–9] Nevertheless, in the case of coal gasification for power generation, Hg removal at high temperatures may lead to improvement in the thermal efficiency of IGCC system. Many researchers deeply investigated the possibility of using noble metals such as gold (Au),[10,11] silver (Ag),[12–14] palladium (Pd)[15,16] and platinum (Pt)[15] as efficient Hg removal sorbents.[17] These Hg removal sorbents, which show excellent performance for removal of Hg, are regenerable and are also stable for long-time operation. Use of noble metals for Hg removal are increasing day by day, that is why knowledge of Hg binding to the surface of metals such as Au, Ag and Pd is very important, especially for the small metal clusters. Granite *et al.*[18] observed that palladium (Pd) offers an attractive method for Hg removal from fuel gas at high temperature, though it would probably require sorbent regeneration to make it cost-effective.

Poulston *et al.*[15] have investigated Hg adsorption capacities of Pt/alumina and Pd/alumina sorbents using a synthetic fuel gas feed containing Hg vapour at temperatures from 204° to 388°C. Both Pt and Pd act as Hg sorbents from fuel gas at temperatures between 204° and 371°C, though Pd was a significantly better sorbent than Pt. An important issue with implementing Pd sorbents in flue and fuel gas environments is dealing with sulphur poisoning. Although the trend is weakly pronounced, previous studies indicate weak binding

*For correspondence

behaviour of sulphur on Pd binary alloys.[19] Lineberry and his co-workers[16] studied capture of Hg from flue gas using injected sorbent of Pd nanoparticle-decorated substrates. They found that palladium-decorated carbon substrates showed excellent mercury capture capabilities, with total efficiencies greater than 90% in laboratory-scale tests. Aboud *et al.*[20] investigated Hg adsorption on some alloys of Pd, namely PdAu, PdAg and PdCu, which are considered as potential candidates for concrete-friendly sorbents. Interestingly, they found that dopant atoms in PdAu, PdAg and PdCu alloys increase adsorption of Hg more effectively when they remain in sub-surface layers.

In terms of theoretical calculations, many researchers[17,21,22] investigated adsorption of elemental Hg on noble metal clusters theoretically. However, to the best of our knowledge, all studies of elemental Hg adsorption are on larger clusters or the 111 and 001 surfaces of noble metals. Nevertheless, most of the active components of dispersed metal catalyst or metal-based sorbents are small-sized clusters, and for their particular characteristics, the cluster properties are mainly responsible.[23,24] Therefore, for a better understanding of chemical, physical and electronic properties such as catalysis effects and adsorption to substrates, a detailed study of adsorption of elemental Hg on small metallic clusters, such as Au_n, Pt_n and Pd_n, is very important.[25] Quantum chemical calculations have already been carried out on small neutral and charged Au[24,26,27], Cu,[28] Pd,[29] Ag,[30–35] Pt, and Rh[25] clusters with adsorbates, such as CO, NO, H_2, O_2 and propene. However, only few theoretical studies of Hg adsorption on small metal clusters[36,37] have been conducted so far. In the present study, density functional theory (DFT) has been used to study the binding of Hg with small neutral and charged Pd_n cluster (n = 1–6), since Pd_n clusters work as a regenerable sorbent in Hg removal experiments.[15,16] To obtain a better insight on the binding mechanism of Hg to neutral and charged Pd_n clusters, we briefly analysed binding energies (BEs), frontier molecular orbitals (FMOs), Mulliken charge and natural bond orbital (NBO) charge.

2. Computational details

Theoretical calculations were carried out utilizing the DFT[38] approach in the Gaussian 03W code.[39] To make the calculations more accurate, a suitable choice of the exchange and correlation functional is needed. Out of various functionals available in Gaussian 03W code,[39] the B3LYP functional[40] was used in the present study. Our choice of B3LYP functional was stimulated by the study of Zanti *et al.*[29] on Pd_n (n = 1–9) clusters. Since Pd is a heavy atom, after consideration of scalar relativistic effects, including mass velocity and Darwin corrections, we used the LANL2DZ basis set and the corresponding Los Alamos relativistic effective core potential (RECP)[41–43], which explicitly consider electrons in the outer orbit through a split valence polarized basis set, thus retaining 18 electrons per Pd atom ($4s^2$ $4p^6$ $4d^{10}$), while the rest of electrons are modelled by an effective core potential taking into account some relativistic corrections (RECP).[41–43] Xiao *et al.*[44] investigated the relativistic effects on geometry and electronic structure of small Pd_n species with the same simulation protocol.

A large number of possible structures were optimized for each size of the cluster, until the minima was obtained on potential energy surface. After the optimization of geometries, vibrational frequencies were also calculated to ensure that these structures were optimized up to true minima. Binding energy (BE) was calculated by the following relation:[45]

$$\mathrm{BE} = E_{\text{cluster-Hg adduct}} - \left(E_{\text{naked cluster}} + E_{\mathrm{Hg}}\right), \quad (1)$$

where the energy of the naked palladium cluster is represented by $E_{\text{naked cluster}}$, energy of Hg molecule is represented by E_{Hg}, and the energy of the naked palladium cluster and adsorbate Hg is represented by $E_{\text{cluster-Hg adduct}}$. Moreover, one can conclude from the above definition that, if the BE is more negative, the interaction will be more strong.

3. Results and discussion

3.1 *Optimized geometries of bare Pd_n clusters and reactivity prediction*

Our literature survey reveals that atomic and electronic structures of small neutral and charged Pd_n clusters have been studied with DFT calculations by many groups.[29,46–50] In this investigation, we have first adapted several initial structures of Pd_n clusters ($2 \leq n \leq 6$) from previous DFT studies[29,46–50] on neutral and charged Pd_n clusters, then we have optimized the geometry of all selected structures. The most stable structures of neutral and charged Pd_n clusters have been represented in figure S1 of the supplementary data. One can observe from figure S1 that the optimized geometries of all Pd_n clusters are in excellent agreement with the geometry reported in literature.[29,46–50]

In order to design a better adsorbent or catalyst and also to reduce computational cost, it is very important to predict the most favourable adsorption site for the

sorbate (which is bare Pd_n cluster in the present investigation).[26] Fukui found an effective approximation for the reactivity prediction using FMO.[52] Reactivity can be predicted with FMO theory by observing interactions between HOMO (highest occupied molecular orbitals) of one species and LUMO (lowest unoccupied molecular orbitals) of the other. Many groups have successfully applied FMO theory for reactivity predictions. Using FMO theory, Wells *et al.*[51] predicted that the most strong interaction of O_2 with the anionic Au_{10} cluster is edge-on attachment to the HOMO of the Au_{10}^- cluster. Recently Joshi *et al.*[45] reported that orientation of adsorbed O_2 can be predicted by frontier molecular orbital picture (FMOP). Adsorption site of CO on small Cu_n ($n = 1$–9) clusters has been predicted by Poater *et al.*[28] using LUMO theory. Furthermore, Chrétien *et al.*[26,34,35] predicted binding of propene with Au_n and Ag_n clusters as well as with their alloy by using LUMO theory. These rules are consistent with the Fukui's FMO theory.[26] Since Hg is an electron donor, thus to study the adsorption of Hg on all neutral and charged Pd_n clusters, we used the rules of LUMOs reported by Chrétien *et al.*[26,34,35] and Poater *et al.*[28] for the reactivity prediction of bare Pd_n clusters. Therefore, HOMOs of Hg and LUMOs of neutral, anionic and cationic Pd_n clusters are the most important molecular orbitals for this study.[28] Figures S2–S4 of supplementary data show the HOMO and LUMO pictures of neutral, cationic and anionic Pd_n clusters. Since all the charged Pd_n clusters are open shell species, there will be two HOMO and two LUMO bearing in mind that in unrestricted formalism, the up and down spins are free to have different spatial orbitals and hence different energies. One is represented as α-HOMO and α-LUMO, while the other one is represented as β-HOMO and β-LUMO. By looking at LUMO pictures of neutral, cationic and anionic

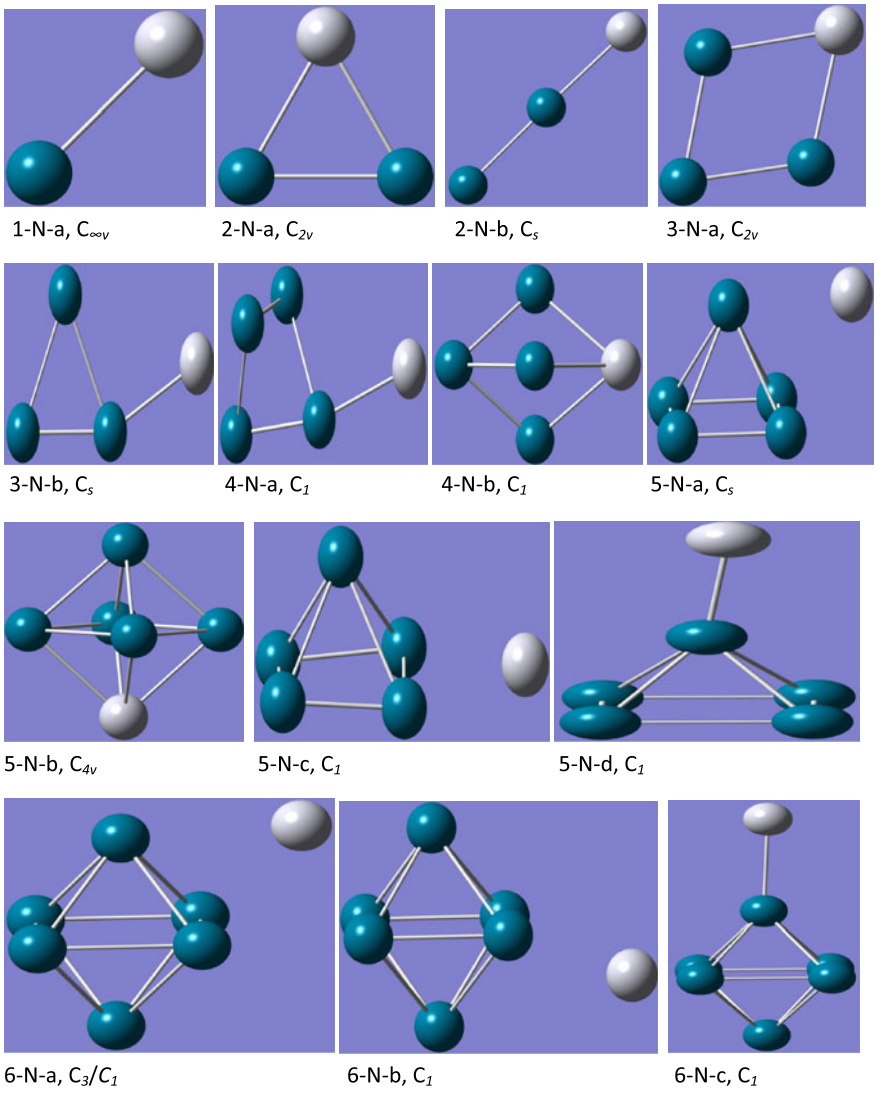

Figure 1. Optimized structures of neutral Pd_nHg complexes, $n \leq 6$. The symmetry point group is indicated.

Pd_n clusters (see figures S2–S4), one can predict that palladium atoms which have larger contributions to the LUMO orbital will be better for adsorption of Hg.[28] For neutral form of Pd_2, the LUMO of Pd dimer exists around both Pd atoms of the naked cluster.[26] On careful observation of the HOMO of Hg molecule and LUMO of bare Pd_2 cluster, one can predict that the bridge type adsorption will be the most favourable. However, there is a possibility of site-on-site adsorption as well. For the equilateral triangle Pd_3 cluster, the external palladium atom would be the most favourable for Hg adsorption. Similarly, for capped triangle Pd_4 cluster, LUMO seems to be equally located around all the Pd atoms. So, there is a strong possibility of site-on-site adsorption for neutral Pd_4 cluster. For neutral Pd_5 and Pd_6 clusters, one can easily conclude by looking into the LUMO picture, that, bridge adsorption is highly expected for both clusters. Similarly, for Pd_2^+ and Pd_3^+ clusters, the β-LUMO has lower MO energy as compared to α-LUMO. Therefore, the most active centre for Hg attack will be the Pd atoms, which have highest contribution in β-LUMO. In case of even anionic Pd_n clusters, we find that MO energy of β-LUMO is lower than MO energy of α-LUMO. It can be predicted that there is very strong possibility of bridge adsorption, although some site-on-site adsorption also seems possible.

Table 1. Calculated data for binding energies (BE, eV) bond distances (Å) and charges on Hg of neutral and charged Pd_nHg complexes.

Species	Adsorption site	Distance of Hg–Pd	BE	Mulliken charge	NBO charge
1-N-a	Top	2.73	−0.619	0.125	0.088
2-N-a	Bridge	2.75	−2.308	0.188	0.234
2-N-b	Top	2.76	−1.653	0.124	0.096
3-N-a	Bridge	2.75	−0.404	0.199	0.337
3-N-b	Top	2.79	−0.392	0.139	0.252
4-N-a	Top	2.84	−0.343	0.111	0.239
4-N-b	Bridge	2.78	−0.243	0.236	0.477
5-N-a	Bridge	3.03	−0.463	0.122	0.298
5-N-b	Bridge	2.79	−0.450	0.278	0.533
5-N-c	Bridge	2.94	−0.448	0.136	0.308
5-N-d	Top	2.85	−0.346	0.125	0.217
6-N-a	Bridge	3.03	−0.516	0.154	0.350
6-N-b	Bridge	2.97	−0.461	0.138	0.324
6-N-c	Top	2.84	−0.369	0.137	0.247
1-C-a	Top	2.75	−1.604	0.414	0.392
2-C-a	Bridge	2.84	−1.734	0.365	0.445
2-C-b	Top	2.80	−1.209	0.276	0.377
3-C-a	Bridge	2.83	−2.282	0.424	0.598
3-C-b	Bridge	2.80	−1.615	0.329	0.525
4-C-a	Bridge	2.85	−0.679	0.363	0.602
4-C-b	Top	2.83	−0.672	0.247	0.433
5-C-a	Bridge	2.97	−1.164	0.252	0.456
5-C-b	Top	2.82	−1.120	0.212	0.413
6-C-a	Bridge	2.96	−1.252	0.231	0.452
6-C-b	Top	2.82	−1.196	0.202	0.405
1-A-a	Top	2.78	−1.174	−0.221	−0.164
2-A-a	Bridge	2.85	−0.540	−0.098	−0.036
2-A-b	Top	2.89	−0.498	−0.116	−0.018
3-A-a	Bridge	2.99	−0.503	−0.057	0.046
3-A-b	Top	2.85	−0.430	0.008	0.069
4-A-a	Bridge	2.92	−0.704	−0.015	0.112
4-A-b	Top	2.79	−0.570	0.038	0.093
5-A-a	Bridge	2.88	−0.797	0.038	0.185
5-A-b	Bridge	3.01	−0.766	0.021	0.186
5-A-c	Top	2.82	−0.477	0.063	0.117
6-A-a	Bridge	2.95	−0.798	0.070	0.253
6-A-b	Bridge	2.89	−0.667	0.047	0.227
6-A-c	Top	2.81	−0.469	0.075	0.144

3.2 *Hg adsorption on the neutral and charged Pd_n clusters*

3.2a *Adsorption of Hg on the neutral Pd_n clusters*: Ground state structures and some low-lying isomers of Pd_nHg complexes have been represented in figure 1. Table 1 represents the BEs and charge on Hg for neutral, cationic and anionic Pd_nHg complexes. In this table, the notation N, C, and A represent the neutral, cationic and anionic clusters, while the notation a, b, c, and d are used for the most stable complex and their low-lying isomers, respectively. In the case of Hg adsorption on single Pd atom, there is only one possibility, which may be called as head-to-head adsorption with $C_{\infty v}$ symmetry. In case of Pd_2Hg (2-N-a) complex, a slight increase has been found in Pd–Pd bond length (from 2.34 Å of naked Pd_2 to 2.76 Å of Pd_2Hg complex). This significant change in Pd–Pd bond length indicates that the adsorption of Hg on bare Pd_2 cluster is very strong. Comparison of figure S1 and figure 1 indicates that the shape of the most stable and some low-lying isomers of neutral Pd_nHg complexes are almost similar (except for Pd_4Hg) to those of the bare Pd_n clusters. Geometry of almost all the neutral Pd_nHg complexes (except for $n = 4$) are either planar or very close-to-planar. It has been observed that the most stable neutral Pd_nHg complexes prefer bridge type adsorption site except the 4-N-a complex. For bridge site adsorption, the average Hg–Pd bond length ranges from 2.75 Å in 2-N-a (in 3-N-a also) to 3.03 Å in 5-N-a (in 6-N-a also), in case of most stable structures (see table 1). It has also been observed that, when the interaction is stronger, the Hg–Pd bond length is shorter. For example, in the case of Pd_2Hg complex, the distance of 2.75 Å between Hg and Pd in bridge type adsorption is the smallest one and BE is highest for Pd_2Hg complex (see figure 2).

3.2b *Adsorption of Hg on the cationic palladium clusters*: Structures of cationic Pd_nHg complexes for the ground state and some low-lying states are represented in figure 3. It can be seen that most of the cationic complexes prefer bridge site adsorption. From figures S1 and 3, it is clear that the geometry of ground state clusters and their less stable isomers are not much affected after Hg adsorption; although some low-lying stable isomers of Pd_nHg complexes also show top site adsorption. Among the given cationic Pd_nHg complexes, almost all of them have similar structures such as bare Pd_n clusters; however, their structures are much different from the neutral Pd_nHg complexes. It can be observed from table 1 and figure 2 that, for the most stable Pd_nHg^+ clusters, the BEs for Hg increases first with the cluster size, then it decreases at one point ($n = 3$ to $n = 4$)) and then again increases.

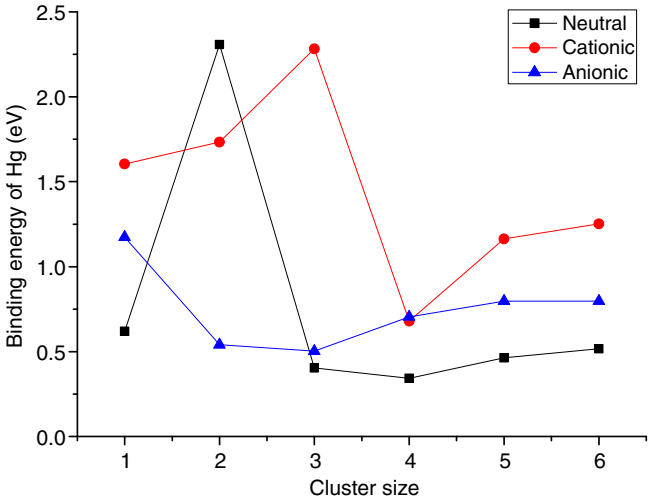

Figure 2. Binding energies as a function of cluster size for Pd_nHg, Pd_nHg^+ and Pd_nHg^- complexes.

3.2c *Adsorption of Hg on the anionic palladium clusters*: Structures of ground state Pd_nHg^- clusters and their less stable isomers are displayed in figure 4. On comparison of figures 4 and S1, one can conclude that these anionic complexes are almost similar to the bare Pd_n clusters like their neutral and cationic forms. For anionic complexes, 'bridge' type adsorption was found to be the most stable. For the most stable Pd_nHg^- complexes from $n = 3$, we find that BEs for Hg adsorption increase with cluster size, and ranges in between 0.503 eV (for 3-A-a) and 1.174 eV (for 1-A-a). BEs are also indicators of charge transfer from adsorbed Hg, since, NBO charge on adsorbed Hg generally increases with increasing BE. BEs of most of the neutral and anionic clusters are smaller than those of cationic Pd_n clusters. Moreover, if BE is above 0.51 eV, attractive force between the adsorbent and adsorbate is very strong and this type of interaction is defined as chemical adsorption. However, if BE is below 0.31 eV, attractive force is relatively weak and is defined as weak chemical adsorption or physical adsorption caused by van der Waals force. From figure 2 and table 1, it is clear that the Hg adsorption on cationic and anionic Pd_n clusters is mainly chemical, while for neutral Pd_n clusters, it is a mixture of chemisorption and physisorption.

3.3 *Validation of reactivity predictors and investigation of some correlations*

Analysis of LUMO indicates that most of the predications have been made accurately. As discussed earlier,

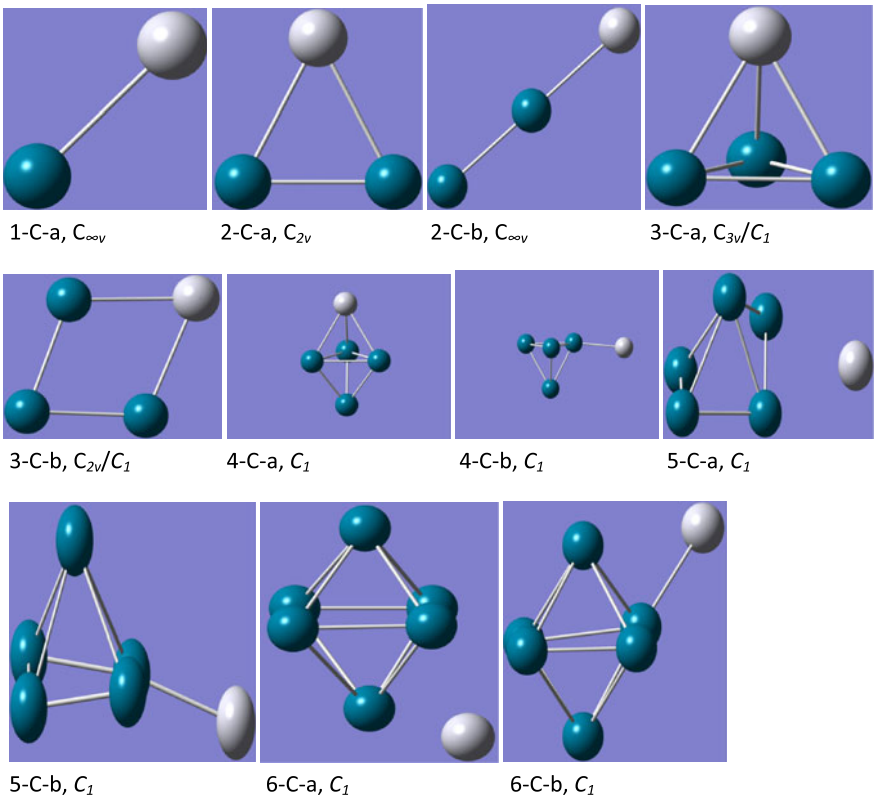

Figure 3. Optimized structures of cationic Pd_nHg complexes, $n \leq 6$. The symmetry point group is indicated.

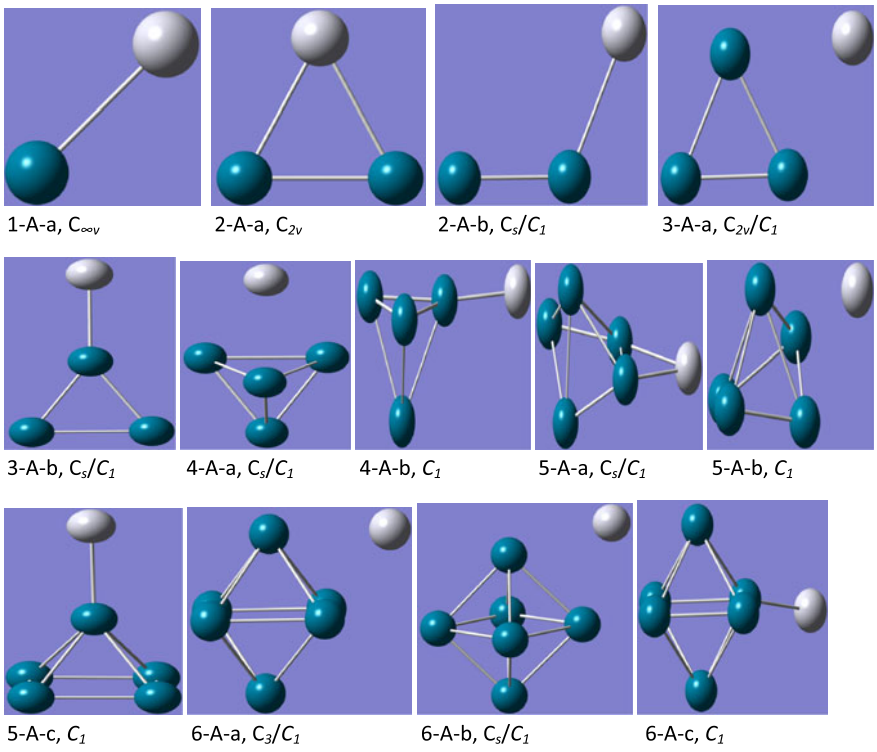

Figure 4. Optimized structures of anionic Pd_nHg complexes, $n \leq 6$. The symmetry point group is indicated.

LUMO of neutral Pd_2 cluster is distributed symmetrically over the bare Pd_2 cluster, which indicates that the Hg atom will be adsorbed to the positions shown in figure 1, which is also supported by our results. Similarly, anionic Pd_2 cluster preferably binds to Hg at the bridge position as predicted by β-LUMO of anionic Pd_2 and HOMO of Hg. The cationic Pd_2 cluster adsorbs Hg with 'bridge' type attraction via β-LUMO of Pd_2^+ and HOMO of Hg. More specifically, for all the neutral, anionic and cationic Pd_n clusters, Hg adsorptions were successfully predicted by these rules.

Since the shape, symmetry and energy order of LUMO is very important[28,34,45] for the adsorption of Hg, BEs should have a close relationship with LUMO energies. We obtained a linear relationship for neutral Pd_n clusters as shown in figure S5 of supplementary data. However, a comparatively poor linear relationship has been found between LUMO energies of cationic Pd_n clusters and BEs for Hg adsorption (see figure S5). However, for anionic Pd_n clusters, a comparatively better linear relationship has been obtained between LUMO energies and BEs, which clearly indicates that neutral and anionic form of Pd_n clusters interact with Hg mainly via the LUMO of Pd_n clusters. For adsorption of propene on small Au_n and Ag_n clusters, almost similar results[28,34,35] were also reported.

Since BEs can also be indicated by charge transfer to the cluster,[45] correlation between BE and NBO/Mulliken charge has also been investigated. In this study, we prefer NBO charges for correlation over Mulliken charges, since, we used a significantly large basis set for Pd and Hg atoms and hence, NBO charges are expected to be more reliable than Mulliken charges.[23] We found an approximate linear correlation between BEs and NBO charges on adsorbed Hg as displayed in figure S6 of supplementary data. In most of the cases, it is observed that greater is the charge transfer to Hg, higher is the value of BE. Moreover, in the present case, BEs and NBO charges show somewhat lower degree of correlation due to a more complicated transfer of electrons in bridge type adsorption. For this type of low degree of correlation, Joshi *et al.*[45] have reported that it is difficult to separate BE contributions of Coulomb attraction, charge transfer to sorbate, back-donation and extent of overlap of relevant orbitals, since all these effects are related to each other in a complex way and operate simultaneously.

Table 2. NBO population analysis for Hg, Pd_4, Pd_4Hg, Pd_4^+, Pd_4Hg^+, Pd_4^- and Pd_4Hg^-.

Species		Pd_1	Pd_2	Pd_3	Pd_4	Hg
Hg	Charges					0.00
	s					2.00
	d					10.00
	p					0.00
Pd_4	Charges	−0.001	0.004	0.001	−0.003	
	s	0.51	0.51	0.51	0.51	
	d	9.41	9.41	9.41	9.42	
	p	0.08	0.08	0.08	0.08	
Pd_4Hg	Charges	0.035↑	0.009↑	0.035↑	−0.318 ↓	0.239↑
	s	0.50	0.51	0.46↓	0.62↑	1.74↓
	d	9.39↓	9.41	9.43↑	9.47↑	9.99
	p	0.08	0.08	0.08	0.23↑	0.02↑
Pd_4^+	Charges	0.252	0.249	0.249	0.250	
	s	0.46	0.46	0.49	0.49	
	d	9.19	9.20	9.17	9.17	
	p	0.10	0.10	0.10	0.10	
Pd_4Hg^+	Charges	0.051↓	0.062↓	0.068↓	0.216↓	0.602↑
	s	0.31↓	0.30↓	0.34↓	0.37↓	1.32↓
	d	9.53↑	9.53↑	9.47↑	9.33↑	9.99
	p	0.12↑	0.12↑	0.13↑	0.09	0.08↑
Pd_4^-	Charges	−0.254	−0.250	−0.249	−0.248	
	s	0.41	0.60	0.60	0.60	
	d	9.78	9.55	9.55	9.55	
	p	0.06	0.09	0.10	0.10	
Pd_4Hg^-	Charges	−0.350 ↓	−0.368 ↓	−0.237 ↑	−0.156 ↑	0.112↑
	s	0.51↑	0.49↓	0.53↓	0.60	1.72↓
	d	9.63↓	9.67↑	9.63↑	9.46↓	10.00
	p	0.21↑	0.21↑	0.08↓	0.10	0.17↑

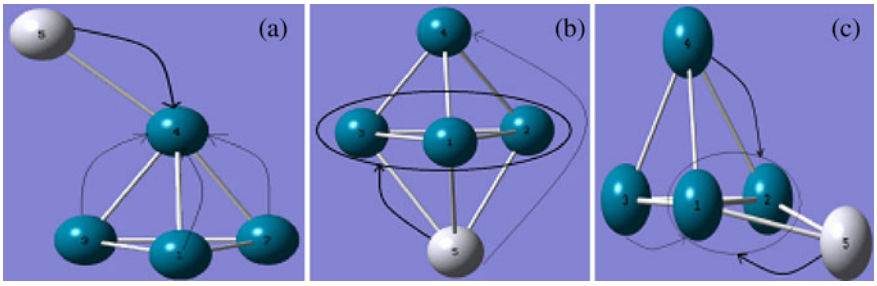

Figure 5. Transfer of electron between Hg and (**a**) neutral Pd_4, (**b**) cationic Pd_4 and (**c**) anionic Pd_4 clusters as observed from NBO analysis.

3.4 *NBO population analysis*

NBO analysis has also been carried out to deeply investigate the tendency of electron transfer between Pd_n clusters and adsorbed Hg. As representative of this investigation, results of ground state structures of neutral and charged Pd_4 and Pd_4Hg clusters are shown in table 2 and figure 5. In case of neutral Pd_4Hg cluster, transfer of charge is from Pd_1, Pd_2, Pd_3 and Hg to the Pd_4, whereas Hg transfers most of the electrons to Pd_4 (dark line in figure 5a) and charge transfer from Pd_1, Pd_2 and Pd_3 is very small (light lines in figure 5a). In cationic Pd_4Hg cluster (figure 5b), mostly charge transfer is from Hg to Pd_1, Pd_2 and Pd_3 (small charge transfer from Hg to Pd_4 also). Charge transfer in anionic Pd_4Hg complex (figure 5c) is from Pd_3, Pd_4 and Hg to Pd_1 and Pd_2, but charge transfer from Pd_3 is significantly small. One can conclude from these results that neutral, anionic and cationic Pd_n clusters are acceptors of electrons. For the Hg atom, s orbital population decreases significantly with slight increase in p orbital population, while almost no change has been observed in d orbital population irrespective of the charge state of the Pd_n cluster. For neutral Pd_nHg clusters, population of Pd atom shows significant change in s and p orbitals, while in d orbital only small change occurs. Population analysis for cationic Pd_nHg clusters shows significant change in population of s and d orbitals, while in p orbital only small change occurs. However, population of s, p and d orbitals shows an observable change for anionic Pd_4Hg cluster. It shows that electron flow in the neutral and charged Pd_4Hg complex is mainly from s orbital of Hg to s, p and d orbitals of Pd.

4. Conclusion

Theoretical study of Hg adsorption on a series of neutral, cationic and anionic Pd_n ($n = 1$–6) clusters has been performed using DFT approach. Findings of this study indicate that the adsorption of Hg is significantly affected by the charged state and size of the cluster. For the neutral Pd_n clusters, BEs of Hg increase first and then decrease and then again increase. A similar pattern has been followed by BEs of Hg with cationic clusters. However, for anionic Pd_n clusters, BEs of Hg first decrease and then increase. Results of NBO analysis indicate that for neutral and charged clusters, mostly electron transfer occurs from s orbital of Hg to s, p and d orbitals of Pd. The rules provided by Chretien *et al.*[26,34,35] have been successfully applied for the prediction of binding site and orientation of Hg with neutral and charged Pd_n clusters. Detailed analysis of final results indicates that, there is a linear relationship between LUMO energies of neutral and charged Pd_n clusters and BEs of Hg.

Supplementary information

Figures S1–S6 can be seen as supporting information at www.ias.ac.in/chemsci: website.

Acknowledgement

We are thankful to the Deanship of Scientific Research for the financial support provided through project Grant no.: NU 45/12, Najran University, Najran, Kingdom of Saudi Arabia.

References

1. Lu D Y, Granatstein D L and Rose D J 2004 *Ind. Eng. Chem. Res.* **43** 5400
2. Liu S, Wang Y, Yu L and Oakey J 2006 *Fuel* **85** 1550
3. Padak B, Brunetti M, Lewis A and Wilcox J 2006 *Environ. Prog.* **25** 319
4. Makkuni A, Varma R S and Sikdar S K 2007 *Ind. Eng. Chem. Res.* **46** 1305
5. Reed G P, Ergudenler A, Grace J R, Watkinson A P, Herod A A, Dugwell D and Kandiyoti R 2001 *Fuel* **80** 623
6. Wu S, Uddin M A and Sasaoka E 2006 *Fuel* **85** 213
7. Portzer J W, Albritton J R, Allen C C and Gupta R P 2004 *Fuel Process. Technol.* **85** 621
8. Lopez-Anton M A, Tascon J M D and Martinez-Tarazona M R 2002 *Fuel Process. Technol.* **77–78** 353

9. Lee J Y, Ju Y, Keener T C and Varma R S 2006 *Environ. Sci. Technol.* **40** 2714
10. Zhao Y X, Mann M, Pavlish J, Mibeck B F, Dunham G and Olson E 2006 *Environ. Sci. Technol.* **40** 1603
11. Baldeck C M, Kalb G W and Crist H L 1974 *Anal. Chem.* **46** 1500
12. Yan T Y 1994 *Ind. Eng. Chem. Res.* **33** 3010
13. Liu Y, Kelly D J A, Yang H Q, Lin C C H, Kuznicki S M and Xu Z H 2008 *Environ. Sci. Technol.* **42** 6205
14. Dong J, Xu Z H and Kuznicki S M 2009 *Environ. Sci. Technol.* **43** 3266
15. Poulston S, Granite E J, Pennline H W, Christina R, Myers C R and Stanko D P 2007 *Fuel* **86** 2201
16. Lineberry Q J, Cao Y, Lin Y, Ghose S, Connell J W and Pan W P 2009 *Energy Fuels* **23** 1512
17. Steckel J A 2008 *Phys. Rev.* **B77** 115412
18. Granite E J, Myers C R, King W P, Stanko D C and Pennline H W 2006 *Ind. Eng. Chem. Res.* **45** 4844
19. Alfonso D R, Cugini A V and Sholl D S 2003 *Surf. Sci.* **546** 12
20. Aboud S, Sasmaz E and Wilcox J 2008 *Main Group Chem.* **7** 205
21. Sasmaz E, Aboud S and Wilcox J 2009 *J. Phys. Chem.* **C113** 7813
22. Zaleski-Ejgierd P and Pyykko P 2009 *J. Phys. Chem.* **A113** 12380
23. Joshi A M, Tucker A M, Delgass W N and Thomson K T 2006 *J. Chem. Phys.* **125** 194707
24. Wu X, Senapati L, Nayak S K, Selloni A and Hajaligol M 2002 *J. Chem. Phys.* **117** 4010
25. Mainardi D S and Balbuena PB 2003 *J. Phys. Chem.* **A107** 10370
26. Chrétien S, Gordon H and Metiu H 2004 *J. Chem. Phys.* **121** 3756
27. Ding X L, Li Z Y, Yang J L, Hou J G and Zhu Q S 2004 *J. Chem. Phys.* **120** 9594
28. Poater A, Duran M, Jaque P, Toro-Labbé A and Solà M 2006 *J. Phys. Chem.* **B110** 6526
29. Zanti G and Peeters D 2009 *Eur. J. Inorg. Chem.* **26** 3904
30. Zhou J, Li Z Y, Wang W N and Fan K N 2006 *J. Phys. Chem.* **A110** 7167
31. Zhao S, Li Z Y, Wang W N and Fan K N 2005 *J. Chem. Phys.* **122** 144701
32. Zhao S, Liu Z P, Li Z H, Wang W N and Fan K N 2006 *J. Phys. Chem.* **A110** 11537
33. Zhou J, Li Z Y, Wang W N and Fan K N 2006 *Chem. Phys. Lett.* **421** 448
34. Chrétien S, Gordon H and Metiu H 2004 *J. Chem. Phys.* **121** 9931
35. Chrétien S, Gordon H and Metiu H 2004 *J. Chem. Phys.* **121** 9925
36. Siddiqui S A, Bouarissa N, Rasheed T and Al-Assiri M S 2013 *Mater. Res. Bull.* **48** 995
37. Lushi S, Anchao Z, Sheng S, Hua W, Junli L and Jun X 2011 *Chem. Phys. Lett.* **517** 227
38. Parr R G and Yang W 1989 *Density functional theory of atoms and molecules* (Oxford: Oxford University Press)
39. Frisch M J *et al.* 2004 Gaussian 03W, Gaussian, Inc.: Wallingford CT
40. Becke B D 1993 *J. Chem. Phys.* **98** 5648
41. Hay P J and Wadt W R 1985 *J. Chem. Phys.* **82** 270
42. Wadt W R and Hay P J 1985 *J. Chem. Phys.* **82** 284
43. Hay P J and Wadt W R 1985 *J. Chem. Phys.* **82** 299
44. Xiao C, Krüger S, Belling T, Mayer M, Rösch N 1999 *Int. J. Quant. Chem.* **74** 405
45. Joshi A M, Delgass W N and Thomson K T 2006 *J. Phys. Chem.* **B110** 23373
46. Zhang W, Ge Q and Wang L 2003 *J. Chem. Phys.* **118** 5793
47. Moseler M, Hakkinen H, Barnett R N and Landman U 2001 *Phys. Rev. Lett.* **86** 2545
48. Zacarias G, Castro M, Tour M and Seminario M 1999 *J. Phys. Chem.* **A103** 7692
49. Nava P, Sierka M and Ahlrichs R 2003 *Phys. Chem. Chem. Phys.* **5** 3372
50. Luo C, Zhou C, Wu J, Kumar T J D, Balakrishnan N, Forrey R C and Cheng H 2007 *Int. J. Quant. Chem.* **107** 1632
51. Wells D H, Delgass W N and Thomson K T 2002 *J. Chem. Phys.* **117** 10597
52. Fukui K, Yonezawa T and Shingu H 1952 *J. Chem. Phys.* **20** 722